1-1-2011

Energy-loss rate of a fast particle in graphene

Yee Sin Ang
ysa190@uowmail.edu.au

Chao Zhang
University of Wollongong, czhang@uow.edu.au

Chun Kee

Recommended Citation

Ang, Yee Sin; Zhang, Chao; and Kee, Chun: Energy-loss rate of a fast particle in graphene 2011, 053111-1-053111-3.
https://ro.uow.edu.au/engpapers/4325

Energy-loss rate of a fast particle in graphene

Yee Sin Ang, C. Zhang, and Chun Yun Kee

Related Articles

Additional information on Appl. Phys. Lett.

Energy-loss rate of a fast particle in graphene

Yee Sin Ang,[1] C. Zhang,[1,a)] and Chun Yun Kee[2]
[1]*School of Engineering Physics, University of Wollongong, 2522 NSW, Australia*
[2]*Department of Mathematics, National University of Singapore, 10 Kent Ridge Crescent, Singapore 119260*

The energy-loss rate of a fast particle in graphene is studied. The energy-loss rate always increases with increasing incident particle energy, which is quite unusual when compared to electron gas in normal metal. Graphene exhibits a "discriminating" behavior where there exists a low energy cut-off below which the scattering process is strictly forbidden, leading to lossless traverse of an external particle in graphene. This low energy cutoff is of the order of nearest neighbor hopping bandwidth. Our results suggest that backscattering is also absent in the external particle scattering of graphene. © 2011 American Institute of Physics. [doi:10.1063/1.3615795]

Graphene is a one-atom thick, 2-dimensional honeycomb structure made up of entirely carbon atoms and was first isolated and characterized in 2004.[1] Graphene is a gapless semiconductor whose valence band touches the conduction band at K and K′ points (commonly known as the "Dirac points") of its Brillouin zone. The interesting aspect of graphene is that the electron at the vicinity of the Dirac points behaves very differently from the usual Schrodinger fermions. At the Dirac points, the effective Hamiltonian can be written compactly as $H = v_F \boldsymbol{\sigma} \cdot \boldsymbol{k}$. This results in a linear energy dispersion $E_k = \pm \hbar v_F k$, and the electrons around the Dirac points instead behaves like a massless ultra-relativistic fermions moving with a reduced "speed of light" $v_F \approx c/300$ ($c =$ vacuum speed of light).[2] It is not surprising that this unique electronic band structure has given rise to many interesting physical phenomena such as the unusually high electron mobility,[3,4] universal conductance,[5–7] half-integer quantum Hall effect,[2,8–10] strong suppression of weak localization,[11–13] and strong nonlinear optical response in the terahertz frequency regime.[14–16]

Electron energy loss spectroscopy (EELS) is a powerful tool which provides physical insights on the electronic band structure, phonon excitation, plasmon excitation, and surface properties of a material. It has recently been utilized in the experimental study of the graphene plasmon properties.[17,18] In order to fully exploit the results of EELS, it is crucial to understand the energy loss rate (ELR) of an external particle in graphene. The ELR of a particle in marginal Fermi liquid[19] and ELR of positron in metal[20] has been theoretically studied. In this work, we extend the formalism in Refs. 19 and 20 to the case of graphene. The ELR of an external particle in an intrinsic ($\mu = 0$) graphene single layer is calculated under the framework of self-consistent field approximation.

We consider a particle with initial momentum $\boldsymbol{p}$, and energy $\varepsilon_{\boldsymbol{p}}$ is fired onto a graphene single layer (see inset of Fig. 1). The particle transfers a momentum of $\Delta \mathbf{p} = \boldsymbol{q}$ and energy $\Delta \varepsilon = \omega = \varepsilon_{\boldsymbol{p}} - \varepsilon_{\boldsymbol{p}-\boldsymbol{q}}$ to the graphene and emerges with a reduced momentum of $\boldsymbol{p} - \boldsymbol{q}$ and energy ε_{p-q} ($\hbar \triangleq 1$). For non-relativistic case, $\omega = pq \cos\phi/m - q^2/2m$, where ϕ is the

angle between $\boldsymbol{p}$ and $\boldsymbol{q}$ and m is the particle mass. The energy loss rate can be written as

$$\frac{d\varepsilon_p}{dt} = \int \frac{d^2q}{(2\pi)^2} W_q(\omega) \tag{1}$$

where $W_q(\omega)$ is the transition probability and is given by

$$W_q(\omega) = \frac{2g_q}{1 - e^{-\beta\omega}} Im\left[\frac{1}{\epsilon_q(\omega)}\right], \tag{2}$$

where g_q is the coupling constant representing the interaction between the incident particle and graphene and β is the inverse temperature $(k_B T)^{-1}$. $\epsilon_q(\omega) = 1 - v_q \Pi(q, \omega)$ is the dielectric function under self-consistent field approximation, where v_q is the strength of electron-electron interaction and $\Pi(q, \omega)$ is the polarizability function of graphene. The imaginary part of the inverse dielectric function in Eq. (2) signifies the incident particle energy-loss in graphene. The polarizability function can be evaluated from the bare bubble diagrams[21] and is given by
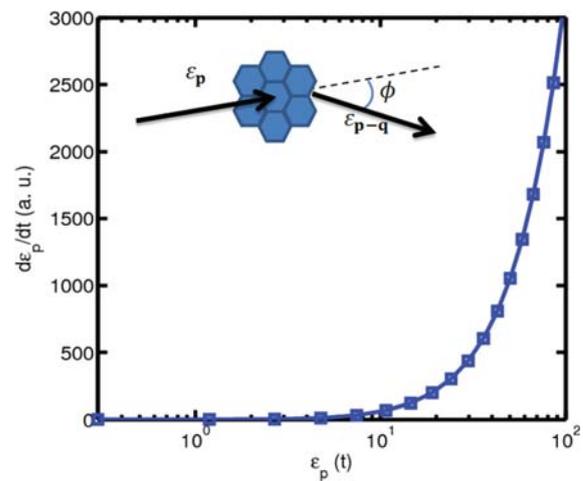

FIG. 1. (Color online) ELR ε_p-sepctrum of electron at T = 77 K. Unlike electron gas in normal metal, graphene ELR always increases with increasing ε_p. The ELR is in the arbitrary unit of $\gamma V_0 \varepsilon_v / \hbar$. Inset shows the scattering process.

$$\prod(q,\omega) = \sum_{k,s,s'} F_{s,s'}(\theta_{k,k+q}) \frac{f_{k+q,s'} - f_{k,s}}{v_F(s'|\boldsymbol{k}+\boldsymbol{q}| - s|\boldsymbol{k}|) - \omega'}, \quad (3)$$

where $\omega' = \omega + i\eta$ with $\eta \to 0$, the wavefunction overlap is $F_{s,s'}(\theta_{k,k+q}) = (1 + ss'\cos\theta_{k,k+q})/2$, where $\theta_{k,k+q}$ is the angle between $\boldsymbol{k}$ and $\boldsymbol{k}+\boldsymbol{q}$ and $f_{k,s}$ is the Fermi-Dirac distribution function with $E_{k,s} = sv_F|\boldsymbol{k}|$, where $s = \pm 1$. The plasmon oscillation has been ignored since it is damped in intrinsic graphene. For intrinsic ($\mu = 0$) graphene at $T = 0$ K, the imaginary polarizability function is given by[21,22]

$$Im[\Pi(q,\omega)] = \frac{1}{4v_F} \frac{q^2}{(\omega^2/v_F^2 - q^2)^{1/2}} \Theta(\omega - qv_F), \quad (4)$$

where both spin and valley degeneracies have been included. Combining Eqs. (1), (2), and (4) and evaluating the integral in polar coordinate, we obtain

$$\frac{d\varepsilon_p}{dt} \propto \int_0^{2\pi} d\phi \int_0^\Lambda \frac{g_q v_q}{|\varepsilon_q(\omega)|^2} \frac{dq}{1 - e^{-\omega\beta}} \frac{q^3\omega}{(\omega^2 - q^2)^{1/2}} \Theta(\omega - q),$$
$$(5)$$

where, for simplicity, yet without losing physics, we have dropped the leading constant terms and denote $\hbar = v_F = k_B = m = 1$. The q-integration is limited by the step-function in Eq. (5). This sets up an upper limit Λ above which the imaginary polarizability function becomes zero.

In order to simplify Eq. (5), we make the following assumptions: (i) the electron-electron interaction is Coulomb, i.e., $v_q = e^2/\varepsilon_0 q$, (ii) the energy loss is small and hence the screening can be treated as static, i.e., $\epsilon_q(\omega) \to \epsilon_q(\omega = 0)$, and (iii) the coupling constant g_q between incident particle and quasiparticle excitation in graphene can be assumed to be of short range and hence is q-independent. It is obvious from Eq. (4) that the static $\epsilon_q(\omega = 0)$ will be contributed solely by the real part of the polarizability function, which can be conveniently evaluated from Eq. (4) using Kramers-Kronig relation[22] and is also q-independent. Finally, we recast Eq. (5) into the following convenient form:

$$\frac{d\varepsilon_p}{dt} = \gamma \frac{V_0 \varepsilon_v}{\hbar} \int_0^{2\pi} \frac{\tilde{\omega}}{1 - e^{-\varepsilon_v\beta'\tilde{\omega}}} d\phi \int_0^\Lambda \frac{\tilde{q}^2 d\tilde{q}}{(\tilde{\omega}^2 - 4\tilde{q}^2)^{1/2}}, \quad (6)$$

where we define $p_0 = mv_F$, $\tilde{q} = q/p_0$, $\tilde{p} = p/p_0$, $\tilde{\omega} = 2\tilde{p}\tilde{q}\cos\phi - \tilde{q}^2$, $\beta' = \beta/2$, $\varepsilon_v = mv_F^2$, $V_0 = e^2/\varepsilon_0 q$, and $\gamma = g/4|\epsilon_0|^2$.

The integration limit Λ can be solved from the step-function in Eq. (5), which gives $\Lambda = 2(\tilde{p}\cos\phi - 1)$. In normal scattering process, the maximum momentum transfer is $2p$, while in graphene the step-function from the imaginary polarizability function has limited the maximum momentum transfer to $2(p - p_0)$. Since nonzero q-integration requires $\Lambda > 0$ or equivalently $p > p_0$, this sets up a critical incident particle energy $\varepsilon_p^c = mv_F/2$, below which the scattering process will be strictly forbidden. This discriminating behavior of graphene is quite unusual. Graphene seems to "discriminate" the incident particle according to their energy and scatter only those with energies higher than ε_p^c, regardless the amount of energy transfer ω. Interestingly, ε_p^c for an

incident electron, is approximately equal to the nearest neighbor hopping bandwidth in graphene $t \approx 2.8$ eV. This implies that a foreign particle with parabolic energy dispersion can travel through without loss of energy.

The ε_p-spectrum is evaluated numerically and plotted in Fig. 1. For electron gas in normal metal, the ELR is known to be proportional to ε_p^c for slow particles and proportional to $\sim \ln(\varepsilon_p)/\varepsilon_p^2$ for fast particles.[20] This, however, does not occur in graphene in which the ELR always increases with increasing ε_p. It is also evident that ELR is zero for $\varepsilon_p < 2.8$ eV. The temperature dependence is generally very weak for particle of all speeds. This is expected since from Eq. (6) the temperature factor carries $\varepsilon_v\beta' \approx 33000$ K/T, which ensures that $[1 - \exp(-\varepsilon_v\beta'\tilde{\omega})]^{-1} \approx 1$ for all moderate temperatures. It is however still obvious that the temperature dependence of slow particle is much stronger than that of the fast particle. Here we should notice two points. (i) The maximum momentum transfer is determined by simultaneous requirement of energy and momentum conservation of the incident electron in the scattering process. Furthermore, the initial and the final state of the graphene are determined by the spectral function of the graphene, given by Eq. (4), which is related to the Dirac fermion nature. Since the scattering involves two particles (the incident electron and the Dirac electron in graphene) the maximum momentum transfer of the incident electron is intrinsically related to the allowed momentum transfer of the Dirac electron. That the back scattering for the Dirac electron in graphene (maximum momentum transfer) is forbidden leads to a reduced maximum momentum transfer of the incident electron. (ii) The dielectric function of the graphene is calculated with the linear energy dispersion approximation, i.e., in the Dirac regime. For this reason the energy transfer in a scattering event between the incident electron and the Dirac electrons should be within the linear regime. This is the case here since the maximum momentum transfer is limited by Λ and p_0 is large. In all figures, different quantities are plotted against the incident energy, not the energy of Dirac electrons.

The ELR is related to mean scattering time τ_p by $\tau_p = \varepsilon_p(d\varepsilon_p/dt)^{-1}$. In Fig. 2, we plot the ε_p-spectrum of the
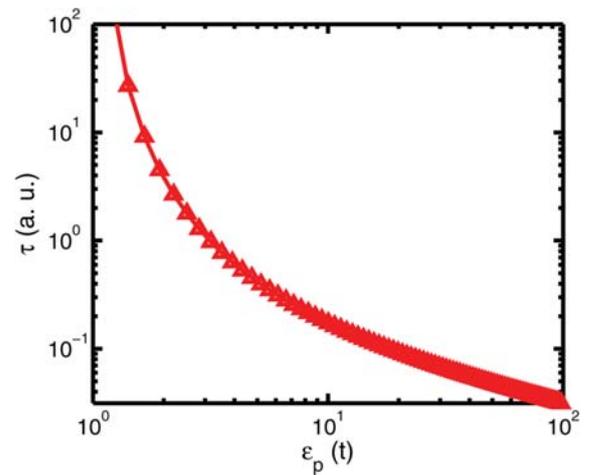

FIG. 2. (Color online) ε_p-spectrum of τ_p at $T = 77$ K. τ_p is plotted in arbitrary unit of $\hbar/2\gamma V_0$.
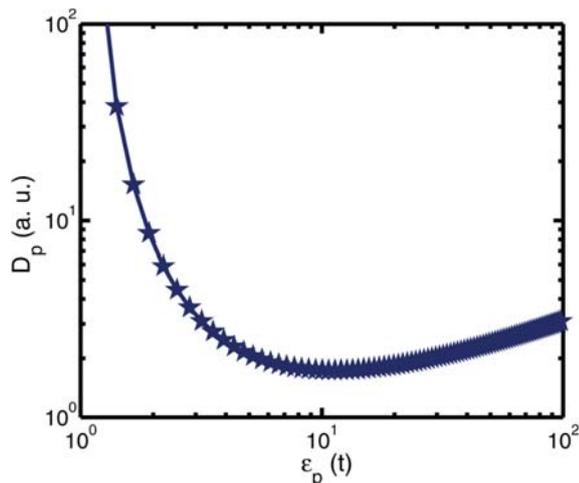
FIG. 3. (Color online) ϵ_p-spectrum of D_p at $T = 77$ K. D_p is plotted in arbitrary unit of $\hbar \epsilon_v / 4\gamma V_0$.

mean scattering time. The temperature dependence is also very weak for the mean scattering time, but, in general, increasing scattering is observed at higher temperatures. τ_p decreases very rapidly with increasing ε_p, indicating energetic particles experience, more profound scatterings in graphene. Note that the low energy tail of the ε_p-spectrum blows up to infinity since it would take almost forever for an extremely slow ($\varepsilon_p \to 0$) particle to be scattered.

The diffusion constant is given by $D_p \sim (mp)^2 \tau_p \sim \varepsilon_p \tau_p$. The ε_p-spectrum D_p is plotted in Fig. 3. In contrast to τ_p, D_p is a non-monotonic function of energy. It is interesting to note that in the high energy regime, there exists a diffusion minimum. The minimum diffusion length is the result of interplay between the incident energy and the scattering time. In the low energy regime $|d\tau_p/d\varepsilon_p| > 1$, and in the high energy regime $|d\tau_p/d\varepsilon_p| < 1$. The boundary of these two distinct energy regimes is $\varepsilon_p \approx 10t$. As a result, there is a diffusion minimum around $\varepsilon_p \approx 10t$.

Finally, we remark that our calculation on the ELR in intrinsic graphene is limited by the temperature dependence of Eq. (4). The step-function-like zero temperature Fermi-Dirac distribution function will be smeared out at finite temperature. The smearing is however quite small and will not significantly alter the results up to temperature in the order of few hundreds K. Therefore, Eq. (4) is reasonably adequate for our current purposes. For higher temperature, where the smearing of the Fermi-Dirac distribution is no longer negligible, the full polarizability function, including both inter- and intraband transitions, should be used.

In conclusion, the energy-loss rate of a charged particle in graphene has been calculated. We present the energy dependence of the energy loss rate, scattering time and the diffusion constant. It is found that slow particles suffer no energy loss at all in graphene. For fast particles, a diffusion minimum has been detected.

[1]K. S. Novoselov, A. K. Geim, S. V. Morozov, D. Jiang, Y. Zhang, S. V. Dubonos, I. V. Grigorieva, and A. A. Firsov, Sicence **306**, 666 (2004).
[2]K. S. Novoselov, A. K. Geim, S. V. Morozov, D. Jiang, M. I. Katsnelson, I. V. Grigorieva, S. V. Dubonos, and A. A. Firsov, Nature **438**, 197 (2005).
[3]K. I. Bolotin, K. J. Sikes, Z. Jiang, M. Klima, G. Fudenberg, J. Hone, P. Kim, and H. L. Stormer, Solid State Commun. **146**, 351 (2008).
[4]J. Chen, C. Jang, S. Xiao, M. Ishigami, and M. Fuhrer, Nat. Nanotechnol. **3**, 206 (2008).
[5]A. B. Kuzmenko, E. van Heumen, F. Carbone, and D. van der Marel, Phys. Rev. Lett. **100**, 117401 (2008).
[6]R. R. Nair, P. Blake, A. N. Grigorenko, K. S. Novoselov, T. J. Booth, T. Stauber, N. M. R. Peres, and A. K. Geim, Science **320**, 1308 (2008).
[7]C. Zhang, L. Chen, and Z. Ma, Phys. Rev. B **77**, 241402 (2008).
[8]Y. Zhang, T. W. Tan, H. L. Stormer, and P. Kim, Nature **438**, 201 (2005).
[9]V. P. Gusynin and S. G. Sharapov, Phys. Rev. Lett. **95**, 146801 (2005).
[10]K. S. Novoselov, Z. Jiang, Y. Zhang, S. V. Morozov, H. L. Stormer, U. Zeitler, J. C. Maan, G. S. Boebinger, P. Kim, and A. K. Geim, Science **315**, 1379 (2007).
[11]H. Suzuura and T. Ando, Phys. Rev. Lett. **89**, 266603 (2002).
[12]S. V. Morozov, K. S. Novoselov, M. I. Katsnelson, F. Schedin, L. A. Ponomarenko, D. Jiang, and A. K. Geim, Phys. Rev. Lett. **97**, 016801 (2006).
[13]D. V. Khveschenko, Phys. Rev. Lett. **97** 036802 (2006).
[14]A. R. Wright, X. G. Xu, J. C. Cao, and C. Zhang, Appl. Phys. Lett. **95**, 072101 (2009).
[15]E. Hendry, P. J. Hale, J. Moger, A. K. Savchenko, and S. A. Mikhailov, Phys Rev. Lett. **105**, 097401 (2010).
[16]X. G. Xu and J. C. Cao, Mod. Phys. Lett. B **24**, 2243 (2010).
[17]T. Eberlein, U. Bangert, R. R. Nair, R. Jones, M. Gass, A. L. Bleloch, K. S. Novoselov, A. Geim, and P. R. Briddon, Phys. Rev. B **77**, 233406 (2008).
[18]J. Lu, K. P. Loh, H. Huang, W. Chen, and A. T. S. Wee, Phys. Rev. B **80**, 113410 (2009).
[19]C. Zhang and Y. Takahashi, Phys. Rev. B **46**, 9247 (1992).
[20]C, Zhang, N. Tzoar, and P. M. Platzman, Phys. Rev. B **37**, 7326 (1988).
[21]E. H. Hwang and S. Das Sarma, Phys. Rev. B **75**, 205418 (2007).
[22]B. Wunsch, T. Stauber, F. Sols, and F. Guinea, New J. Phys. **8**, 318 (2006).